

DOI: 10.1002/((please add manuscript number))

**Article type: Communication**

## **Formation of liquid-liquid micropatterns through guided liquid displacement on liquid-infused surfaces**

*Dorothea Paulssen,<sup>1</sup> Wenqian Feng,<sup>1</sup> Ivana Pini,<sup>1</sup> and Pavel A. Levkin<sup>1,2\*</sup>*

<sup>1</sup>Institute of Toxicology and Genetics (ITG), Karlsruhe Institute of Technology (KIT), 76344 Eggenstein-Leopoldshafen, Germany

<sup>2</sup>Institute of Organic Chemistry, Karlsruhe Institute of Technology (KIT), 76021 Karlsruhe, Germany

\*levkin@kit.edu

**Keywords:** slippery surfaces, imbibition, liquid displacement, surface patterning, droplet microarrays

**Abstract:** Here we demonstrate a method to pattern liquids of varying surface tension and composition into droplets by utilizing slippery liquid-infused surfaces prepared on chemically-patterned substrates. We study the capability of different liquids to displace the lubricant from higher surface energy regions and show that both high and low surface tension liquids can imbibe the polymer, thereby forming droplets sharply following underlying surface energy patterns. For all liquids tested, droplet arrays of arbitrary shapes of each liquid were formed with precision down to 50  $\mu\text{m}$ . By changing the chemical patterning from fluorinated to aliphatic groups, patterns of mineral and silicone oils were created. Finally, we demonstrate formation of two-dimensional micropatterns of three-phase liquid systems – fluorinated, organic, and aqueous phases.

Liquid patterning on solid surfaces is an essential process in micro- and nano-fabrication. It has been used for microelectromechanical systems (MEMS)-fabrication,<sup>[1],[2],[3]</sup> microfluidic-device design<sup>[4],[5]</sup> bio-scaffold creation,<sup>[6]</sup> or high-throughput screening efforts.<sup>[7],[8],[9],[10],[11]</sup> It is usually accomplished by applying liquids via a highly controlled method such as contact or

non-contact printing,<sup>[12],[13],[14],[15],[16]</sup> pre-structured surfaces,<sup>[17],[18],[19]</sup> micropatterning through thin liquid film instabilities<sup>[20],[21]</sup> or wettability patterning such as superhydrophobic-hydrophilic patterns.<sup>[22]</sup> The latter example enables the formation of patterns of aqueous solutions using the effect of discontinuous de-wetting process.<sup>[17, 23], [24], [25]</sup>

How liquids spread on a surface is determined by their surface tension relative to the surface tension of the solid at the contact line of the three phase system.<sup>[26], [27]</sup> Thus, low surface tension liquids, such as perfluorinated oils (e.g. perfluoropolyether), silicone oils, and many organic solvents can easily wet different materials<sup>[28]</sup>, while liquids with higher surface tension often form confined droplets. Several methods were recently developed that enable patterns of low surface tension liquids using the effect of discontinuous de-wetting.<sup>[24], [29]</sup> Tuteja et al. introduced a method requiring superoleophobic-superoleophilic patterns,<sup>[23, 30]</sup> while the approach of Feng et al. relies on the formation of defect-free surfaces to create patterns of regions with strong de-wettability towards organic solvents.<sup>[31]</sup> Neither of those methods, however, enables patterning of liquids with extremely low surface tensions below 18 mN/m. To pattern such liquids, including fluorinated or silicone oils, “double-re-entrant” topographies<sup>[28, 30]</sup> are required. However, these do not prevent liquids from spreading laterally once in contact with these features.<sup>[32]</sup>

Another problem is that aqueous solutions containing proteins, lipids, sugars or other biological components derived from cells, cell lysates or growth medium, may not only possess lower surface tensions but can also hydrophilize surfaces by adsorbing biomolecules, thereby degrading the liquid repellent character of such surfaces.<sup>[33], [34], [35], [36], [37]</sup> For this reason, formation of complex surface patterns of organic solvents or biofluids remains difficult.

Liquid-infused interfaces or slippery surfaces possessing excellent liquid repellence were recently introduced by impregnating a nano/micro-structured or porous surface with a lubricant, thereby creating a stable lubricant layer on top of this surface.<sup>[38], [39], [40], [41], [42], [43]</sup> A favourable disjoining pressure maintains a stable lubricant film on the surface.<sup>[44], [45], [46]</sup> In

contrast to air-filled repellent surfaces, such liquid-locked surfaces reveal greater robustness against pressure and hydrodynamic shear<sup>[47]</sup>. There is evidence that slippery surfaces are superior in anti-fog, anti-icing, and anti-biofouling applications<sup>[42], [48], [37], [22]</sup> to traditional hydro- and omniphobic or polyethylene glycol-functionalized (PEGylated) surfaces.

Here, we demonstrate that the displacement of one lubricant liquid by another liquid depends on the underlying substrate's surface chemistry. We show that by patterning the substrate with superhydrophobic/hydrophilic features we can control the liquid-liquid displacement process spatially. This process can be used to spontaneously form micropatterns of liquid droplets with surface tensions ranging from 72 mN/m (water) down to <18 mN/m (*n*-hexane). In addition, by forming surface patterns of fluorinated, alkylated and hydroxylated regions, it was possible to create three phase patterns using fluorinated, organic and aqueous fluids.

Fabrication of superhydrophobic-hydrophilic patterned surfaces was performed using the following approach (Figure 1A).<sup>[49]</sup> First, a 15  $\mu\text{m}$  thin porous poly(2-hydroxyethyl methacrylate-*co*-ethylene dimethacrylate) (HEMA-EDMA) layer with pore sizes ranging from 80 nm to 250 nm<sup>[50]</sup> was polymerized on a glass slide. The polymer layer can be rendered superhydrophobic (SH) (advancing water contact angles  $\theta_{adv} = 170^\circ \pm 2$  receding water contact angles  $\theta_{rec} = 157^\circ \pm 0.5$ ) or hydrophilic ( $\theta_{adv} = 46^\circ \pm 5$  and  $\theta_{rec} = 0^\circ$ ) through the esterification with 4-pentynoic acid (alkylated surface) and the UV-induced thiol-yne reaction with *1H,1H,2H,2H*-perfluorodecane-1-thiol (PFDT) or  $\beta$ -mercaptoethanol, respectively. The polymer film can be patterned via sequential UV-induced thiol-yne reactions with the aid of quartz photomasks.<sup>[49]</sup> Previously, this method has reported to yield patterns with sizes as small as 10  $\mu\text{m}$  and below.<sup>[49]</sup>

The wetting abilities of both fluorinated PFDT-modified and hydrophilic HEMA-EDMA surfaces were investigated with a set of liquids with different surface tensions ranging from 16 mN/m to 72 mN/m (Tables 1). The PFDT-modified polymer was non-wettable for liquids with

surface tensions higher than  $\sim 40$  mN/m (Figure 2) and the liquid droplets remained in the Cassie's state.<sup>[51]</sup> However, it was wetted by liquids with surface tension below 40 mN/m, such as ethanol, DMF as well as by low-surface tension lubricants Krytox GPL 103 (PFPE) (20 mN/m), silicone oil (20.1 mN/m) or mineral oil (32 mN/m). On the other hand, high-surface energy hydrophilic porous HEMA-EDMA could be infused by all liquids studied (Table 1).

Surprisingly, there is a difference in contact angle values for PFDT and CH3 substrates infused with the same PFPE lubricant (Table 1). A possible explanation is the presence of defects on the lubricant-infused surfaces that leads to exposed substrate and to such differences in contact angles. In addition, the number of defects should depend on the type of surface functionality, thereby making such liquid-infused surfaces even more different.

The roughness of the porous HEMA-EDMA layer and its capillary network are key to forming stable liquid-infused surfaces and liquid-liquid patterns. On a smooth surface, exposing perfluorodecanethiol (PFDT) functional groups (see Feng et al.),<sup>[31]</sup> PFPE cannot be stabilized and does not form a stable liquid layer. On the rough PFDT-modified HEMA-EDMA surface, however, stable PFPE liquid layers can be formed. 'Slipperiness' of a surface is characterized by low contact angle hysteresis or low sliding angles.<sup>[40], [37]</sup> The sliding angles of different liquids on PFPE-lubricated PFDT-modified HEMA-EDMA are small enough to classify this lubricant-infused surface as slippery and the contact angle hysteresis (CAH) were also significantly reduced. Organic solvents (e.g. hexane, ethanol, toluene, dichloromethane, dimethyl formamide, DMSO) exhibited sliding angles around  $5^\circ$  (Table 3) and CAH values were reduced to around  $10^\circ$  (Figure 2A).

We then investigated the ability of different liquids to spontaneously replace PFPE impregnating hydrophilic porous HEMA-EDMA lubricant. We found that all studied liquids could replace PFPE from the pores of the hydrophilic polymer (Table 2). Lower surface tension liquids, such as ethanol and DMSO, pinch more readily to the underlying surface (Video S1). It took around 15 to 20 seconds for water to pinch on a PFPE-lubricated surface (Video S3),

while it took only around 1s for ethanol to replace the lubricant on this surface (Video S1 and S1). The replacement took place even by liquids less dense than that of PFPE.

Krummel et al.<sup>[52]</sup> as well as Datta et al.<sup>[53]</sup> demonstrated that the complete displacement of oil in a porous substrate through the wetting fluid is achievable provided the capillary number (the relative effect of viscous forces versus surface tension) rises above a certain threshold value. We observed that when a solvent was applied on a patterned SLIPS, the lubricant was displaced from the hydrophilic pattern (see Figure S1 and S2). Thus, cells could be grown in the hydrophilic patterns from which lubricant had been replaced (see Figure S3). Interestingly, after the evaporation of the solvent, PFPE did not flow into the dried hydrophilic features again (but in a reverse pattern PFPE features would flow out into dried background – see Video S5) if access PFPE had been removed with an air gun prior to the experiment. On the other hand, PFPE lubricant could not be replaced by any of the used liquid from the PFDT-modified regions. The exception was hexane. Even though it did not wet PFPE-infused PFDT-borders, when wetting dried features with hexane, small PFPE droplets were pulled from the borders into the hexane phase (see Figure S2 and Video S4). However, *n*-hexane would stay confined to the hydrophilic features (see Figure 1 and S4).

By combining superhydrophobic PFDT-modified with hydrophilic porous polymer regions in the same surface it becomes possible to achieve spatially controlled selective de-wetting of the PFPE lubricating liquid by different solvents (Figure 1). Such patterned surfaces can serve as a template for an array of high and low surface tension liquids.<sup>[54]</sup> As shown in Figure 1, porous HEMA-EDMA patterned with either hydrophilic (HL) or fluorinated (PFDT-modified) regions is completely wetted with PFPE lubricant. However, the PFPE oil is displaced from the HL parts (and not from the PFDT areas) after introducing a secondary liquid, such as *n*-hexane, silicone oil, ethanol, water, DMSO, etc. (Figure 1B-D) This leads to a binary liquid-liquid pattern of the higher surface tension liquid in HL parts and lower surface tension liquid in the PFDT-regions. Thus, by a simple, two-step process, non-miscible liquids can be spatially

arranged into precise two-dimensional compartments (Figures 1, S1). The homogeneity of heights of droplets was measured by sliding a 100  $\mu$ L droplet down a 30°-inclined pattern of hydrophilic 3 mm circles in a PFDT-background, and measuring the heights of 10 droplets. The heights of glycerol, DMSO, n-hexadecane droplets varied by 0.1%, 4.8%, and 3.5%, respectively (Figure S3). Droplets could be formed both on features of several millimetre in diameter as well as on small features down to 40  $\mu$ m in width (see Figure S5).

Modifying HEMA-EDMA with dodecanethiol<sup>[49]</sup> instead of PFDT by a thiol-yne click reaction created a hydrophobic but non-fluorinated surface with advancing and receding WCAs being 154 $\pm$ 2 and 82 $\pm$ 4, respectively, as well as 85 $\pm$ 3 and 0 CAs for DMSO. However, the alkylated porous surface allowed the formation of slippery surfaces with oil types other than the perfluoro lubricants (Figures 3B, 4). When infused with either silicone or mineral oils, dodecanethiol-modified HEMA-EDMA exhibited a stable lubricant film that could not be washed off with water or even perfluoro oils. On both oil-infused surfaces, non-miscible liquids (such as water and on silicone oil DMSO) exhibited roll-off and hysteresis angles close to 0 (Table 2). However, while silicone oil-infused surfaces were slippery for perfluorocarbon solvents such as PFPE and FC40 as reported elsewhere,<sup>[43]</sup> mineral oil-infused surfaces were not. Perfluorinated oils would readily wet and spread on mineral oil-infused dodecanethiol-modified HEMA-EDMA (Table 2). Thus, spatially controlled droplets of PFPE and FC40 could be created using silicone oil-infused borders (Figure 3 and Figure S6). In contrast to higher surface tension liquids, PFPE droplets varied in height by 25% when formed on PFDT-modified 3 mm diameter circles in a dodecanethiol-modified background (Figure S5).

The ability to pattern any two liquids on the same substrate next to each other has various applications, e.g. in liquid-liquid extractions,<sup>[55]</sup> chemical process design,<sup>[56], [57]</sup> and microfabrication research, such as tuneable micro-lenses<sup>[58], [59]</sup> to list a few. One of the applications is to use such liquid patterning to stably position an oil shield around an aqueous compartment to avoid evaporation of small aqueous reservoirs. Aqueous droplets evaporate fast

on an open surface if not protected from the environment. To circumvent this problem, droplets can be covered by a layer of oil. However, shielding droplets via a continuous oil layer can lead to cross-contamination between aqueous compartments<sup>[60]</sup>. Instead, it is advisable to shield each droplet via an individual oil layer not connected to neighbouring aqueous compartments. To realize this, HL circles (1.5 mm in diameter) were surrounded by alkylated SH 4 mm wide rings, which was again surrounded by PFDT-modified borders (Figure 4). The surface was then covered with a PFPE layer, followed by a sequential replacement of the fluorinated oil from the hydrophilic spots by water and then from the alkylated rings by a mineral oil to form aqueous compartments in the hydrophilic spots covered by individual mineral oil droplets kept fixed on the surface with the alkylated rings. Thus, a three-phase array of water-in-oil-droplets separated by a slippery PFPE-infused surface was created (Figure 4). Such arrays of shielded aqueous compartments can have applications, for example, in DNA sequencing, related nucleotide operations,<sup>[61]</sup> enzymatic assays and protein crystallization,<sup>[19], [62], [63]</sup> as well as in cellular assays requiring long term stability of water droplets. The water-oil structures were kept stable by the surrounding slippery PFPE border for at least 4 weeks. Figure 4 demonstrates the ability of such a system to significantly reduce evaporation of aqueous droplets even after heating the sample at 100°C for 5 minutes.

In conclusion, we demonstrate that by choosing the appropriate chemical surface patterning, liquid-liquid displacement can be spatially controlled for a wide range of lubricant-intruding liquid pairs. Arrays of both high and low surface tension liquids can thus be formed on a single surface. Spontaneous formation of droplet microarrays on slippery lubricant-infused surfaces prepatterned with matching surface chemistry was shown. The resulting arrays of an intruding liquid follow precisely the underlying surface patterning with, for example, circular, square or other geometries. By modifying the same porous polymer surface with patterns of aliphatic alkyl groups, hydroxy and perfluoro groups, three-phase liquid micropatterns – fluoro, organic, aqueous – could be formed. This approach demonstrates the potential of three immiscible

liquids being patterned adjacently in arbitrary droplet shapes, as long as the matching lubricant-intruding liquid pair and corresponding surface chemistries have been chosen. This flexibility carries enormous potential for the miniaturization of various processes where liquids of varying surface tensions need to be patterned, confined or manipulated on surfaces or in channels.

### **Experimental Part.**

2-Hydroxyethyl methacrylate, ethylene dimethacrylate, 2,2,3,3,3-pentafluoropropyl methacrylate (PFPPMA), trichloro(1H, 1H, 2H, 2H-perfluorooctyl)silane, 2,2-dimethoxy-2-phenylacetophenol, benzophenone, cyclohexanol, 1-decanol, rhodamine B, mineral oil, were purchased from Sigma-Aldrich (Taufkirchen, Germany) at purity >97%.

Krytox GPL 103 was purchased from DuPont (Hamm, Germany). FC40 as well as PicoSurf2™ were supplied by Dolomite Microfluidics (Royston, UK). Quartz photomask was developed with Autodesk Inventor 2011 software and manufactured by Rose Fotomasken (Bergisch Gladbach, Germany). Glass plates were obtained from Schott Nexterion (Mainz, Germany). All other chemicals were purchased from Carl Roth (Karlsruhe, Germany).

*Hydrophobic/hydrophilic Patterned Surface Fabrication:* glass slides were activated by submerging in 1M NaOH for 30 min followed by thorough rinsing with mQ H<sub>2</sub>O. Then slides were left in 1M HCl for 1 h and rinsed with water again. After drying, slides were modified by a 20% (v/v) 3-(trimethoxy silyl)propyl methacrylate (Sigma-Aldrich) in ethanol. To avoid the formation of air bubbles, 70 µL modification solution was evenly applied twice between the active sites of two glass slides for 30 min. Glass slides were washed with acetone. Fluorinated glass slides were prepared for the manufacturing of polymer surface. For this, activated glass slides were incubated overnight in a vacuumed desiccator in the presence of trichloro(1H, 1H, 2H, 2H-perfluorooctyl)silane.



Polymerization solution consisted of polymers (24% wt. 2-hydroxyethyl methacrylate as monomer and 16% wt. ethylene dimethacrylate as a cross-linker) as well as initiator (1% wt. 2,2-dimethoxy-2-phenylacetophenone) dissolved in 1-decanol (12% wt.) and cyclohexanol (48% wt.). 60  $\mu\text{L}$  polymerization mixture was pipetted onto modified glass slides. These were then covered by fluorinated glass slides separated through 15  $\mu\text{m}$  silica bead spacers from modified glass slides. Slides were irradiated for 15 min with 5.0 to 4.0  $\text{mW}\cdot\text{cm}^{-2}$ , 260 nm UV-light. The mould was then carefully opened using a scalpel and polymer washed for at least 2h in ethanol.

Hydrophilic polymer surfaces were esterified by immersion of 2 slides in 50 mL dichloromethane containing 4-pentynoic acid (111.6 mg, 1.14 mmol) and catalyst 4-(dimethylamino)pyridine (DMAP) (56 mg, 0.46 mmol) at  $-20^{\circ}\text{C}$ . After 20 min, 180  $\mu\text{L}$  coupling reagent N,N'-diisopropylcarbodiimide (DIC) was added and the solution stirred at room temperature for at least 4h or overnight. Esterified slides were washed in ethanol for 2h.

Patterning of esterified slides was based on photomask lithography. Slides were irradiated either with “superhydrophobic” or “hydrophilic” click-chemistry solution first under the pattern of choice, followed by washing with acetone and drying. In a second step, slides were wetted with the complementary solution, covered with a quartz slide and irradiated with UV.

Superhydrophobic click-chemistry solution 1 was prepared always fresh by dissolving 10% vol./vol. 1H,1H,2H,2H-perfluorodecanethiol in ethyl acetate. Hydrophilic solution 2 consisted of 2-mercaptoethanol (10% vol./vol.) dissolved in a 50:50 vol./vol. ethanol/water mix.

In the first patterning step, slides were wetted with 200  $\mu\text{L}$  solution 1 in the dark. Slides were covered by the desired photomask pattern and irradiated for 2 min ( $5.0 \text{ mW}\cdot\text{cm}^{-2}$ , 260 nm). After irradiation slides were rinsed twice with acetone in the dark. They were wetted with solution 2 and covered by a quartz slide. Immediately after, slides were irradiated for 2 min by UV again ( $5.0 \text{ mW}\cdot\text{cm}^{-2}$ , 260 nm) and subsequently washed for at least 2 h in ethanol before use.

*SEM images.* Patterned HEMA-EDMA slides were coated with gold particles and images were taken using a thermal field emission SEM using a FE-REM (type Merlin, Zeiss).

*Contact and Sliding Angle Measurements:* 60  $\mu\text{L}$  of PFPE were applied and allowed to spread evenly for all contact and sliding angle measurements. In case any other lubricant was used equally 60  $\mu\text{L}$  of lubricant was spread on the surface. To obtain surfactant-spiked PFPE, a 2% wt./wt. stock solution of PicoSurf2<sup>TM</sup> (Dolomite, Royston, UK) dissolved in FC40 was mixed 1:3 with pure PFPE solution, and the FC40 was allowed to evaporate.

Advancing and receding contact angles (for Figure 2) were determined by an inhouse-build system encompassing an UK1117 camera (EHD imaging GmbH, Damme, Germany), a stage and 5  $\mu\text{L}$  syringe (Hamilton, Bonaduz, Switzerland) connected to a pump operating at stable flow speed (15  $\mu\text{L}/\text{min}$ ). Images were taken at 100 ms per frame. Contact angles were measured using the ImageJ plug-in DropSnake.<sup>[64], [65]</sup> For each condition measured, 3 slides were used, and advancing/receding angles were measured on 5 different position on each chip. Sliding angles were determined manually on an adjustable angle stage. For table 2, advancing and receding contact angles were measured 3 times on 2 different surfaces using Krüss contact angle goniometer (Hamburg, Germany). For this liquid was either flushed from or sucked into the syringe at a rate of 2.67  $\mu\text{L}/\text{min}$  and videos were recorded.

*Cell Culture:* Human Cervical tumour cell line HeLa expressing GFP was purchased from BioCat (Heidelberg, Germany). Cell lines were cultured in DMEM (Gibco, Life Technologies GmbH, Darmstadt, Germany), supplemented with 10% (vol./vol.) FBS (Sigma), and 1% of Penicillin/Streptomycin (Gibco, Life Technologies GmbH, Darmstadt, Germany). Additionally, HeLa growth medium was supplemented with 0.2% G418 (Gibco, Life Technologies GmbH, Darmstadt, Germany). Cells were cultured at 37°C in a humidified atmosphere of CO<sub>2</sub> and 95% air. The cultured cells were observed with inverted light microscope (CKX 31 Olympus, Japan). Once cells covered ~75-80% of the culture dish, they were trypsinized using 0.25% trypsin/EDTA (Gibco, Life Technologies GmbH, Darmstadt,

Germany) and diluted in fresh medium – using a blood cell counting chamber (Neubauer, celceromics, Cambridge, UK) – to a density of  $15\text{--}20 \times 10^3$  cells/cm<sup>2</sup>.

For seeding onto superhydrophobically/hydrophilically patterned HEMA-EDMA lubricated with surfactant-spiked PFPE, a drop of cell containing medium was slid over patterns; small parts of medium attached to hydrophilic spots, thus, forming micro-droplets of cell-containing growth medium. Alternatively, a large drop of 500  $\mu\text{L}$  was laid over several hydrophilic spots and allowed to rest in order that cells could sediment down. After 30 seconds, the array slide was tilted allowing excess liquid to flow off. Fluorescent images were taken with Keyence BZ-9000 fluorescent microscope (Osaka, Japan).

*Microscopic Imaging:* All microscopic bright field images and videos were taken with Keyence BZ-9000 fluorescent microscope (Osaka, Japan).

### **Supporting Information**

Supporting Information is available from the Wiley Online Library or from the author.

### **Acknowledgements**

The research was supported by the ERC Starting Grant (DropCellArray 337077), ERC Proof-of-Concept grant (CellPrintArray 768929) and the HGF-ERC-0016 grant from the Helmholtz Associations' Initiative and Networking Fund. The authors would also like to thank William Jefferson for taking photographs (C-F) in Figure 1, and Jiaqi Guo for taking photograph (H) in Figure 1. Finally, we would like to thank Udo Geckle (IAM/KIT) for taking the SEM image displayed in supplementary Figure S4.

### **References**

- [1] J. Z. Wang, Z. H. Zheng, H. W. Li, W. T. S. Huck, H. Siringhaus, *Nat. Mater.* **2004**, 3, 171.
- [2] H. A. Biebuyck, G. M. Whitesides, *Langmuir* **1994**, 10, 2790.
- [3] X. Bi, W. Li, *J. Mater. Chem. C* **2015**, 3, 5825.

- [4] D. A. Bruzewicz, M. Reches, G. M. Whitesides, *Anal. Chem.* **2008**, 80, 3387.
- [5] I. You, T. G. Lee, Y. S. Nam, H. Lee, *ACS Nano* **2014**, 8, 9016.
- [6] A. I. Neto, K. Demir, A. A. Popova, M. B. Oliveira, J. F. Mano, P. A. Levkin, *Adv. Mater.* **2016**, 28, 7613.
- [7] A. a. J. J. J. You, Rebecca and M. Whitesides, George and L. Schreiber, Stuart, *Chemistry & biology* **1998**, 4, 969.
- [8] E. Ueda, P. A. Levkin, *Adv. Healthcare Mater* **2013**, 2, 1413.
- [9] J. Bruchmann, I. Pini, T. S. Gill, T. Schwartz, P. A. Levkin, *Adv. Healthcare Mater* **2017**, 6, 1601082.
- [10] W. Feng, L. Li, C. Yang, A. Welle, O. Trapp, P. A. Levkin, *Angew. Chem.* **2015**, 54, 8732.
- [11] W. Feng, E. Ueda, P. A. Levkin, *Adv. Materials*, 0, 1706111.
- [12] P. Calvert, *Chem. Mater.* **2001**, 13, 3299.
- [13] S. A. Massimo Mastrangeli, Cagdas Varel, Christiaan van Hoof, Jean-Pierre Celis, KF Böhlinger, *J. Micromech. Microeng.* **2009**, 19.
- [14] R. E. Saunders, B. Derby, *Int. Mater. Rev.* **2014**, 59, 430.
- [15] D. Qin, Y. Xia, J. A. Rogers, R. J. Jackman, X.-M. Zhao, G. M. Whitesides, in *Microsystem Technology in Chemistry and Life Science*, (Eds: A. Manz, H. Becker), Springer Berlin Heidelberg, Berlin, Heidelberg **1998**, 1.
- [16] D. B. Weibel, W. R. Diluzio, G. M. Whitesides, *Nat Rev Microbiol* **2007**, 5, 209.
- [17] R. J. Jackman, D. C. Duffy, E. Ostuni, N. D. Willmore, G. M. Whitesides, *Anal. Chem.* **1998**, 70, 2280.
- [18] P. Angenendt, L. Nyarsik, W. Szaflarski, J. Glökler, K. H. Nierhaus, H. Lehrach, D. J. Cahill, A. Lueking, *Anal. Chem.* **2004**, 76, 1844.
- [19] Y. Zhu, L.-N. Zhu, R. Guo, H.-J. Cui, S. Ye, Q. Fang, *Sci. Rep.* **2014**, 4, 5046.
- [20] A. Verma, A. Sharma, *Adv. Mater.* **2010**, 22, 5306.

- [21] D. C. Hyun, M. Park, U. Jeong, *J. Mater. Chem. C* **2016** 2016, 4, 10411.
- [22] E. Ueda, P. A. Levkin, *Adv Mater* **2013**, 25, 1234.
- [23] E. Ueda, F. L. Geyer, V. Nedashkivska, P. A. Levkin, *Lab Chip* **2012**, 12, 5218.
- [24] S. P. R. Kobaku, A. K. Kota, D. H. Lee, J. M. Mabry, A. Tuteja, *Angew. Chem.* **2012**, 51, 10109.
- [25] S. P. R. Kobaku, G. Kwon, A. K. Kota, R. G. Karunakaran, P. Wong, D. H. Lee, A. Tuteja, *ACS Appl. Mater. Interfaces* **2015**, 7, 4075.
- [26] W. A. Zisman, in Contact Angle, Wettability, and Adhesion, Vol. 43, *American Chemical Society*, **1964**, 1.
- [27] J. E. D Bonn, J. Indekeu, J. Meunier, E. Rolley, *Rev Mod. Phys.* **2009**, 81 739
- [28] T. L. Liu, C. J. Kim, *Science* **2014**, 346, 1096.
- [29] Y.-K. Lai, Y.-X. Tang, J.-Y. Huang, F. Pan, Z. Chen, K.-Q. Zhang, H. Fuchs, L.-F. Chi, *2013*, 3, 3009.
- [30] A. Tuteja, W. Choi, G. H. McKinley, R. E. Cohen, M. F. Rubner, *MRS Bulletin* **2011**, 33, 752.
- [31] L. L. W Feng, X Du, A Welle, PA Levkin, *Adv. Mater.* **2016**, 28, 3202.
- [32] R. Almeida, J. W. Kwon, *Langmuir* **2013**, 29, 994.
- [33] B. Lassen, K. Holmberg, C. Brink, A. Carlén, J. Olsson, *Colloid Polym. Sci* **1994**, 272, 1143.
- [34] W. Norde, *Macromolecular Symposia* **1996**, 103, 5.
- [35] a. M Mrksich, G. M. Whitesides, *Annu. Rev. Biophys. Biomol. Struct.* **1996**, 25, 55.
- [36] R. A Latour, in *Encyclopedia of biomaterials and biomedical engineering*, (Ed: W. G. Bowlin GL), Marcel Dekker, New York **2008**.
- [37] A. Grinthal, J. Aizenberg, *Chem. Mater.* **2014**, 26, 698.
- [38] T.-S. Wong, S. H. Kang, S. K. Y. Tang, E. J. Smythe, B. D. Hatton, A. Grinthal, J. Aizenberg, *Nature* **2011**, 477, 443.

- [39] A. Lafuma, D. Quéré, *EPL* **2011**, 96, 56001.
- [40] N. Vogel, R. A. Belisle, B. Hatton, T. S. Wong, J. Aizenberg, *Nat Commun* **2013**, 4, 2167.
- [41] A. Eifert, D. Paulssen, S. N. Varanakkottu, T. Baier, S. Hardt, *Adv. Mater.Interfaces* **2014**, 1.
- [42] J. Li, T. Kleintschek, A. Rieder, Y. Cheng, T. Baumbach, U. Obst, T. Schwartz, P. A. Levkin, *ACS Appl Mater Interfaces* **2013**, 5, 6704.
- [43] F. Schellenberger, J. Xie, N. Encinas, A. Hardy, M. Klapper, P. Papadopoulos, H. J. Butt, D. Vollmer, *Soft Matter* **2015**, 11, 7617.
- [44] J. Cui, D. Daniel, A. Grinthal, K. Lin, J. Aizenberg, *Nat Mater* **2015**, 14, 790.
- [45] D. Daniel, J. V. I. Timonen, R. Li, S. J. Velling, J. Aizenberg, *Nat Phys* **2017**, 13, 1020.
- [46] L. W. Schwartz, R. R. Eley, *J. Colloid Interface Sci.* **1998**, 202, 173.
- [47] C. Howell, T. L. Vu, C. P. Johnson, X. Hou, O. Ahanotu, J. Alvarenga, D. C. Leslie, O. Uzun, A. Waterhouse, P. Kim, M. Super, M. Aizenberg, D. E. Ingber, J. Aizenberg, *Chem. Mater.* **2015**, 27, 1792.
- [48] L. Xiao, J. Li, S. Mieszkin, A. Di Fino, A. S. Clare, M. E. Callow, J. A. Callow, M. Grunze, A. Rosenhahn, P. A. Levkin, *ACS Appl Mater Interfaces* **2013**, 5, 10074.
- [49] W. Feng, L. Li, E. Ueda, J. Li, S. Heißler, A. Welle, O. Trapp, P. A. Levkin, *Adv. Mater.Interfaces* **2014**, 1, 1400269.
- [50] K. Kreppenhofer, J. Li, R. Segura, L. Popp, M. Rossi, P. Tzvetkova, B. Luy, C. J. Kähler, A. E. Guber, P. A. Levkin, *Langmuir* **2013**, 29, 3797.
- [51] A. B. D. Cassie, S. Baxter, *T Faraday Soc* **1944**, 40, 546.
- [52] A. T. D. Krummel, S. S. ; Muenster, S. ; Weitz, D. A., *Aiche Journal* **2013**, 59, 1022.
- [53] S. S. Datta, T. S. Ramakrishnan, D. A. Weitz, *Phys. Fluids* **2014**, 26, 022002.
- [54] Q. Z. B Chang, RHA Ras, A Shah, Z Wu, K Hjort, *Appl. Phys. Lett.* **2016**, 108

- [55] V. Jokinen, R. Kostianen, T. Sikanen, *Adv. Mater.* **2012**, 24, 6240.
- [56] M. D. Scanlon, A. Berduque, J. Strutwolf, D. W. M. Arrigan, *Electrochimica Acta* **2010**, 55, 4234.
- [57] F. Marken, J. D. Watkins, A. M. Collins, *Phys. Chem. Chem. Phys.* **2011**, 13, 10036.
- [58] L. Dong, H. Jiang, *Appl. Phys. Lett.* **2006**, 89, 211120.
- [59] L. Dong, A. K. Agarwal, D. J. Beebe, H. Jiang, *Adv. Mater.* **2007**, 19, 401.
- [60] P. Gruner, B. Riechers, B. Semin, J. Lim, A. Johnston, K. Short, J.-C. Baret, *Nat. Commun.* **2016**, 7, 10392.
- [61] A. V. Almeida, A. Manz, P. Neuzil, *Lab Chip* **2016**, 16, 1063.
- [62] G. Arrabito, F. Cavaleri, V. Montalbano, V. Vetri, M. Leone, B. Pignataro, *Lab Chip* **2016**, 16, 4666.
- [63] Y. Sun, X. Chen, X. Zhou, J. Zhu, Y. Yu, *Lab Chip* **2015**, 15, 2429.
- [64] A. F. Stalder, G. Kulik, D. Sage, L. Barbieri, P. Hoffmann, *Colloids and Surfaces A: Physicochemical and Engineering Aspects* **2006**, 286, 92.
- [65] A. F. Stalder, T. Melchior, M. Müller, D. Sage, T. Blu, M. Unser, *Colloids and Surfaces A: Physicochemical and Engineering Aspects* **2010**, 364, 72.
- [66] Surface tension values of some common test liquids for surface energy analysis. Vol. **2017**; Available from: <http://www.surface-tension.de/>.
- [67] S. Ross, VARIATION WITH TEMPERATURE OF SURFACE TENSION OF LUBRICATING OILS, **1950**, Available from: <http://www.dtic.mil/dtic/tr/fulltext/u2/a801538.pdf>.
- [68] I. Clearco Products Co., Vol. **2017**, Available from: <http://www.clearcoproducts.com/pdf/low-viscosity/NP-PSF-10cSt.pdf>.
- [69] X. He, W. Qiang, C. Du, Q. Shao, X. Zhang, Y. Deng, *Journal of Materials Chemistry A* **2017**, 5, 19159.

[70] 3M™, 3M™ Heat Transfer Fluids, Vol. **2017**, Available from:

<http://multimedia.3m.com/mws/media/65495O/3mtm-thermal-management-fluids.pdf>.

FIGURES



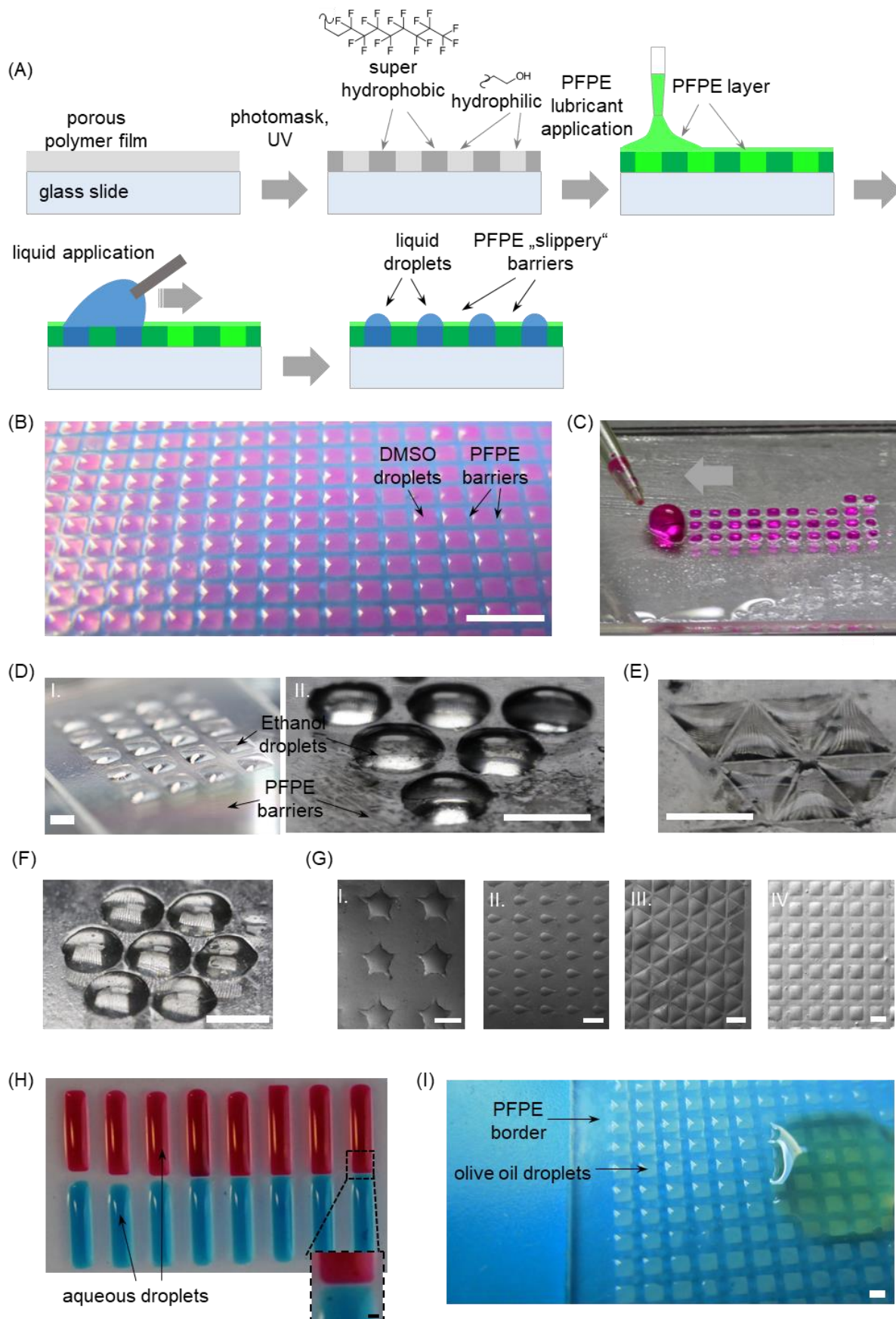


Figure 1. Strategy for liquid patterning on porous poly(2-hydroxyethyl methacrylate-co-ethylene dimethacrylate) (HEMA-EDMA) polymer. A) Schematic representation of the

manufacturing process of surface patterned HEMA-EDMA and subsequent infusion with liquids into defined compartments. B) Photographs of an array where hydrophilic patterns are differentially wetted with rhodamine-containing DMSO, while superhydrophobic borders are wetted with a perfluorinated oil (PFPE). (C) Photograph of the production of such an array by discontinuous de-wetting. Images of ethanol droplets (D) (scale bar corresponds to 3 and 2 mm respectively), silicone oil droplets (E) (scale bar corresponds to 1 mm), mineral oil (F) (scale bar corresponds to 2 mm), and N-hexane (G) droplets (scale bars correspond to 350  $\mu\text{m}$ , 350  $\mu\text{m}$ , 350  $\mu\text{m}$  and 1 mm) formed on hydrophilic patterns of different shapes. (H) Photograph of water droplets stained with food dyes separated by small borders – the smallest just being 50  $\mu\text{m}$ . The water droplets were formed on a surface lubricated with surfactant-spiked PFPE (see Materials and Methods). (I) Photograph of mineral oil drops formed on hydrophilic spots within a PFPE background – the scale bar corresponds to 1 mm.

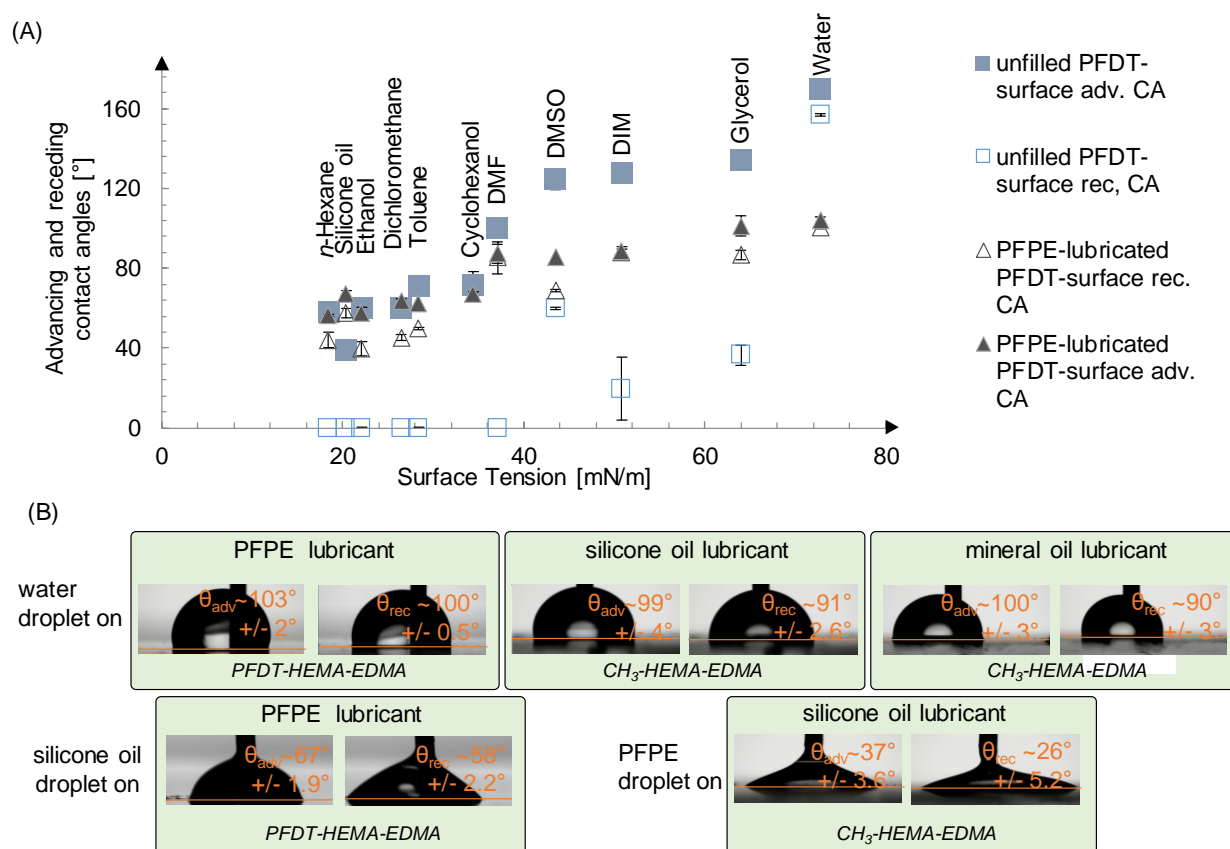


Figure 2. Change in material properties through lubrication with oil. A) Change in advancing and receding angles of surfaces between dry state and upon and upon lubrication with PFPE for standard liquids. B) Advancing and receding angles of water (upper row) as well as silicone oil/ PFPE (lower row) on alkylated poly(2-hydroxyethyl methacrylate-co-ethylene dimethacrylate) polymer lubricated by either mineral oil (right) or silicone oil (middle) or perfluorinated and lubricated by PFPE (left).

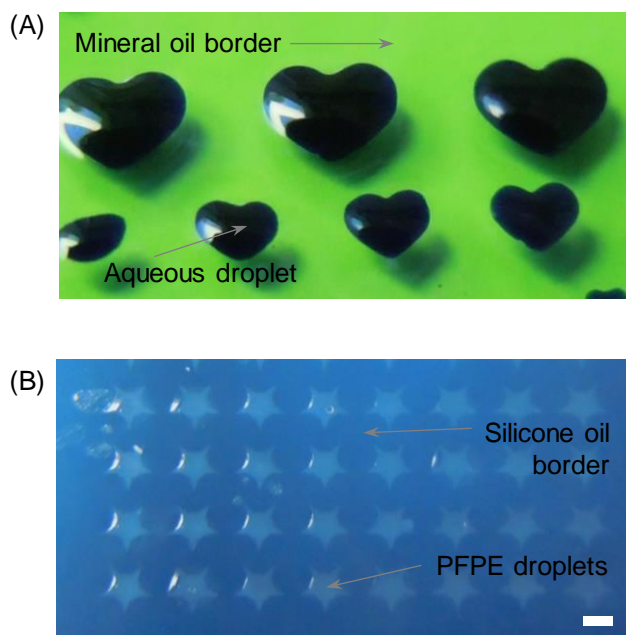


Figure 3. Droplet formation on alkylated surfaces. (A) aqueous droplets formed on mineral oil-lubricated alkylated polymer. (B) PFPE droplets formed on silicone oil-lubricated alkylated polymer. Scale bars represent 1 mm.

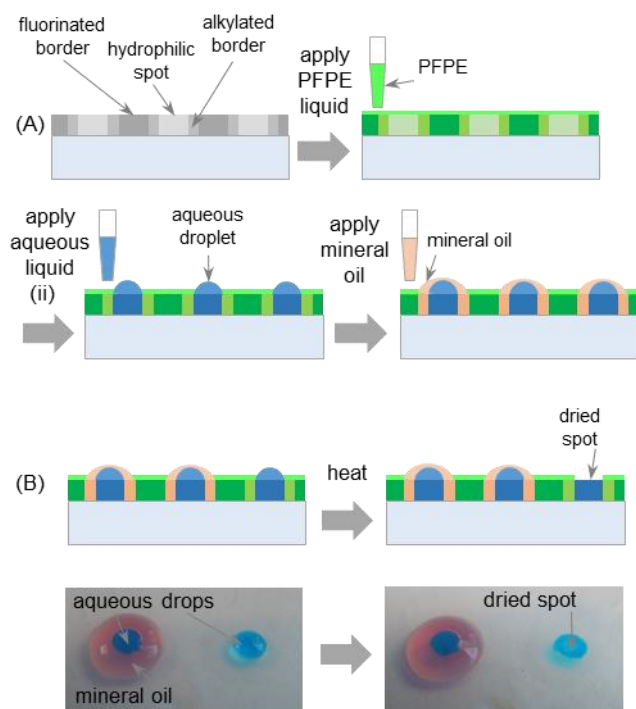


Figure 4. Formation of evaporation resistant compartments. A) Schematic representing the three-phase system enabled through surface patterning of perfluorinated, alkylated and hydrophilic patches next to each other. B) Photographs of mineral oil protected droplet next to an unprotected droplet before (left) and after (right) heating.

**TABLES.**

Table 1 List of tested liquids

Table 1 List of tested liquids

Liquid Name	Surface tension [mN/m] @ 20°C	Density [g/cm <sup>3</sup> ] @ 20°C
Water	72 <sup>[66]</sup>	0.998
Glycerol	64 <sup>[66]</sup>	1.261
Diiodomethane (DIM)	50.8 <sup>[66]</sup>	3.325
DMSO	43.54 <sup>[66]</sup>	1.1004
Dimethylformamide (DMF)	37.10 <sup>[66]</sup>	0.948
Cyclohexanol	34.4 (at 25°C) <sup>[66]</sup>	0.9624
Mineral oil light bioreagent	32 <sup>[67]</sup>	0.8
Toluene	28.40 <sup>[66]</sup>	0.87
<i>n</i> -Hexadecane	27.5 <sup>[66]</sup>	0.77
Dichloromethane	26.5	1.3266
Ethanol	22.10 <sup>[66]</sup>	0.810
Silicone oil 10 cSt	20.1 (at 25°C) <sup>[68]</sup>	0.95
Krytox GPL 103 (PFPE)	20 <sup>[69]</sup>	1.88
<i>n</i> -Hexane	18.43 <sup>[66]</sup>	0.6606
FC40	16 <sup>[70]</sup>	1.855

Table 2. Overview of tested combinations between lubricant, surface patterning and intruding liquid.

Infusing liquid	Water	Mineral Oil			Silicone Oil			PFPE		
	OH	PFDT	CH <sub>3</sub>	OH	PFDT	CH <sub>3</sub>	OH	PFDT	CH <sub>3</sub>	OH
Intruding liquid										
<b>PFPE</b>	$\theta_{adv}$ 0 $\theta_{rec}$ 0	d	$\theta_{adv}$ 0 $\theta_{rec}$ 0	$\theta_{adv}$ 0 $\theta_{rec}$ 0	d	$\theta_{adv}$ 37 $\theta_{rec}$ 26	$\theta_{adv}$ 34 $\theta_{rec}$ 31	-	-	-
<b>Silicone oil</b>	$\theta_{adv}$ 0 $\theta_{rec}$ 0	d	d	d	-	-	-	$\theta_{adv}$ 67 $\theta_{rec}$ 58	d	d
<b>Mineral oil</b>	$\theta_{adv}$ 0 $\theta_{rec}$ 0	-	-	-	$\theta_{adv}$ 40 $\theta_{rec}$ 0	$\theta_{adv}$ 29 $\theta_{rec}$ 0	$\theta_{adv}$ 30 $\theta_{rec}$ 0	$\theta_{adv}$ 74 $\theta_{rec}$ 50	d	d
<b>Cyclohexanol</b>	$\theta_{adv}$ 0 $\theta_{rec}$ 0	Miscible	Miscible	Miscible	$\theta_{adv}$ 26 $\theta_{rec}$ 13	$\theta_{adv}$ 50 $\theta_{rec}$ 42	d	$\theta_{adv}$ 67 $\theta_{rec}$ 48.5	d	d
<b>Water</b>	-	$\theta_{adv}$ 101 $\theta_{rec}$ 60	$\theta_{adv}$ 100 $\theta_{rec}$ 90	d	$\theta_{adv}$ 113 $\theta_{rec}$ 81	$\theta_{adv}$ 99 $\theta_{rec}$ 91	d	$\theta_{adv}$ 103 $\theta_{rec}$ 100	$\theta_{adv}$ 121 $\theta_{rec}$ 83	d

d = displacement of the infused liquid by the intruding liquid;

$\theta_{\text{adv}}$  = advancing contact angle of the intruding liquid on a corresponding liquid-infused surface;

$\theta_{\text{rec}}$  = receding contact angle of the intruding liquid on a corresponding liquid-infused surface;  
 Hydroxylated: OH; Perfluorinated: PFDT; Alkylated: CH<sub>3</sub>; Standard deviations can be found in supplementary information.

Table 3. Sliding angles of solvents on PFDT-functionalized, PFPE-infused HEMA EDMA

<i>Liquid Name</i>	<i>Sliding angle [°]</i>
Water	4.85 ± 0.35
Glycerol	6.34 ± 0.5
Diiodomethane (DIM)	4.36 ± 0.25
DMSO	4.49 ± 0.52
Dimethylformamide (DMF)	4.85 ± 0.17
Cyclohexanol	5.38 ± 0.0.53
Mineral oil light - bioreagent	4.9 ± 0.14
Toluene	3.81 ± 0.35
Dichloromethane	4.42 ± 0.26
Ethanol	5.25 ± 0.61
Silicone oil 10 cSt	4.37 ± 0.4
<i>n</i> -Hexane	5.44 ± 0.5

**Keyword: slippery surfaces, imbibition, liquid displacement, surface patterning, superhydrophobicity, droplet microarrays**

Dorothea Paulssen,<sup>1</sup> Wenqian Feng,<sup>1</sup> Ivana Pini,<sup>1</sup> and Pavel A. Levkin<sup>1,2\*</sup>

**Formation of liquid-liquid micropatterns through guided liquid displacement on liquid-infused surfaces**

ToC figure

